

Supporting Information

Gas-Phase Lanthanide Chloride Clusters: Relationships among ESI Abundances and DFT Structures and Energetics

Philip X Rutkowski,[†] Maria C. Michelini,^{‡,*} and John K. Gibson^{†,*}

[†]*Chemical Sciences Division, Lawrence Berkeley National Laboratory, Berkeley, CA 94720, USA*

[‡]*Dipartimento di Chimica, Università della Calabria, Via P. Bucci, Cubo 14 C, 87030 Arcavacata di Rende, Italy*

Table of contents

Figures S1a-n. ESI mass spectra of 350 μM LnCl_3 in isopropanol. LnCl_{3n+1}^- clusters are labeled. (Ln = La – Lu, with the exception of Pm).

Figure S2. ESI mass spectra of 140 μM LaCl_3 and 100 μM LuCl_3 in isopropanol.

Figure S3. ESI mass spectra of 350 μM LaCl_3 and LuCl_3 in isopropanol with a chloride ion concentration of 10.35 mM.

Figure S4. Geometric structures of higher-energy isomers of La_2Cl_7^- and Lu_2Cl_7^- .

Figure S5. Different views of $\text{La}_6\text{Cl}_{19}^-$ showing different lanthanide coordination numbers.

Figure S6. Portion of ESI mass spectrum of a solution of 350 μM TmCl_3 in 1% $\text{D}_2\text{O}/99\%$ $(\text{CH}_3)_2\text{CH}(\text{OD})$ showing $\text{Tm}_3\text{Cl}_{10}^-$ and its hydration and hydrolysis products. For each species the three m/z peaks calculated as most intense are indicated by arrows.

Figure S7. Hydration and hydrolysis products of La_2Cl_7^- and $\text{La}_3\text{Cl}_{10}^-$.

Figures S8a-f. ESI mass spectra of LnBr_3 in isopropanol. LnBr_{3n+1}^- clusters are labeled. (Ln = La, Ce, Pr, Nd, Sm, Lu).

Figures S9a-b. ESI mass spectra of LnI_3 in isopropanol. LnI_{3n+1}^- clusters are labeled. (Ln = La, Lu).

Table S1. Atoms in Molecules (AIM) charges for LaCl_3 and $\text{La}_n\text{Cl}_{3n+1}^-$ (n = 1- 6) clusters.

Table S2. Atoms in Molecules (AIM) charges for LuCl_3 and $\text{Lu}_n\text{Cl}_{3n+1}^-$ (n = 1-6) clusters.

Table S3. Lanthanide bromide cluster abundances summed for all isotopic contributions.

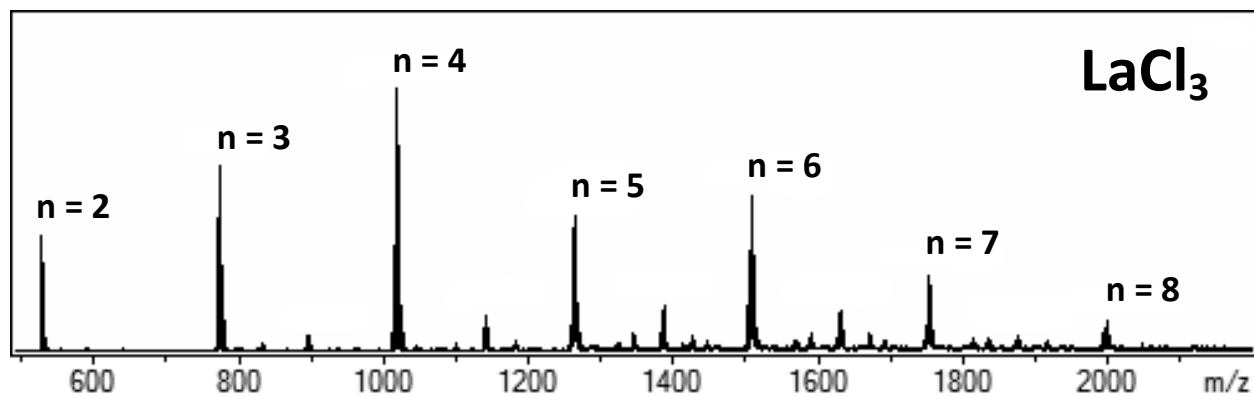


Figure S1a. ESI mass spectra of 350 μM LaCl₃ in isopropanol. La_nCl_{3n+1}⁻ clusters are labeled.

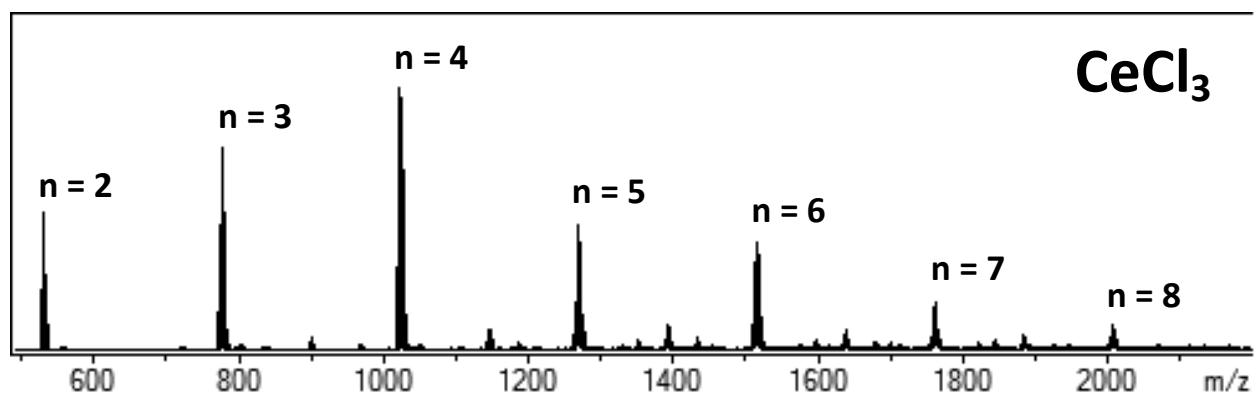


Figure S1b. ESI mass spectra of 350 μM CeCl₃ in isopropanol. Ce_nCl_{3n+1}⁻ clusters are labeled.

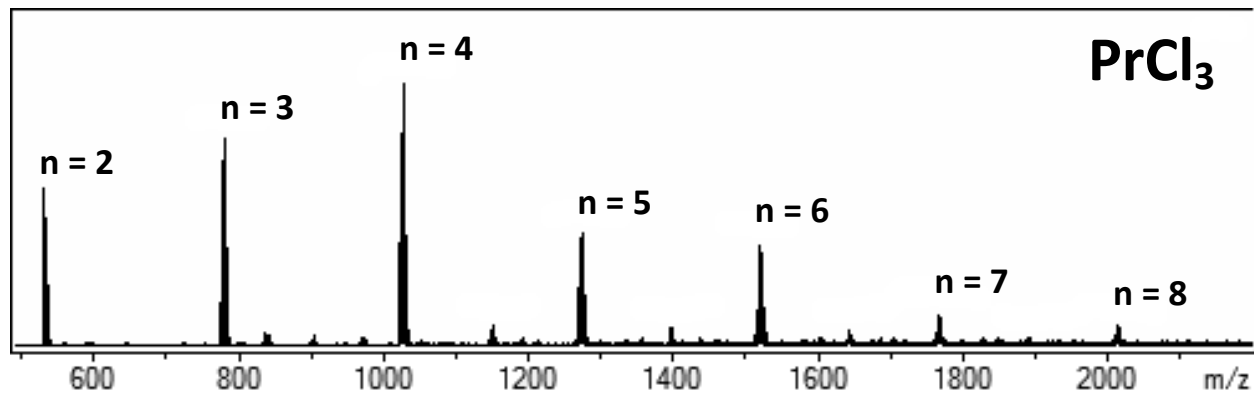


Figure S1c. ESI mass spectra of 350 μM PrCl₃ in isopropanol. Pr_nCl_{3n+1}⁻ clusters are labeled.

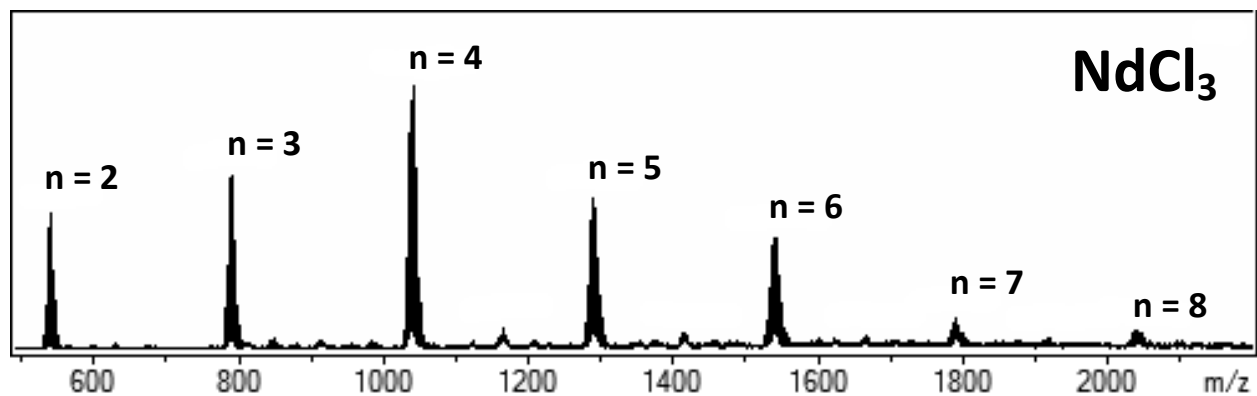


Figure S1d. ESI mass spectra of 350 μM NdCl_3 in isopropanol. $\text{Nd}_n\text{Cl}_{3n+1}^-$ clusters are labeled.

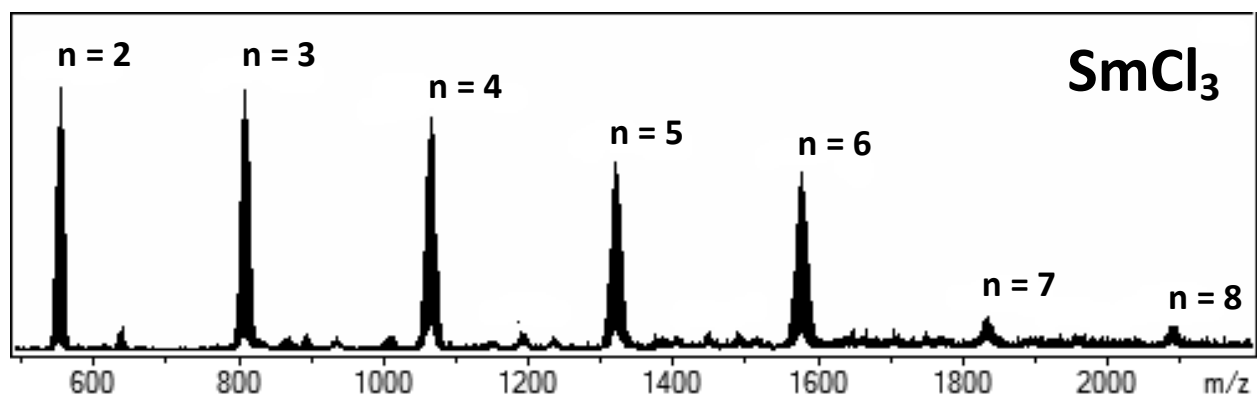


Figure S1e. ESI mass spectra of 350 μM SmCl_3 in isopropanol. $\text{Sm}_n\text{Cl}_{3n+1}^-$ clusters are labeled.

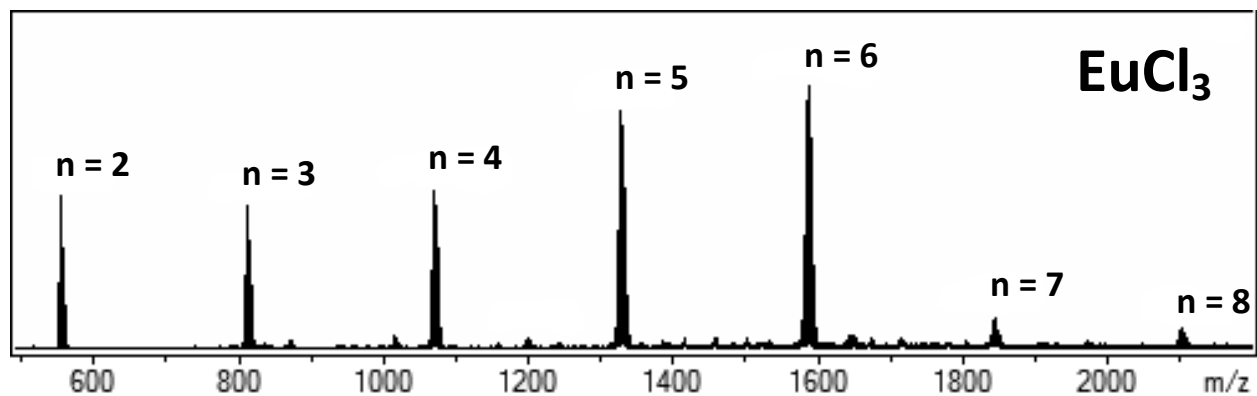


Figure S1f. ESI mass spectra of 350 μM EuCl_3 in isopropanol. $\text{Eu}_n\text{Cl}_{3n+1}^-$ clusters are labeled.

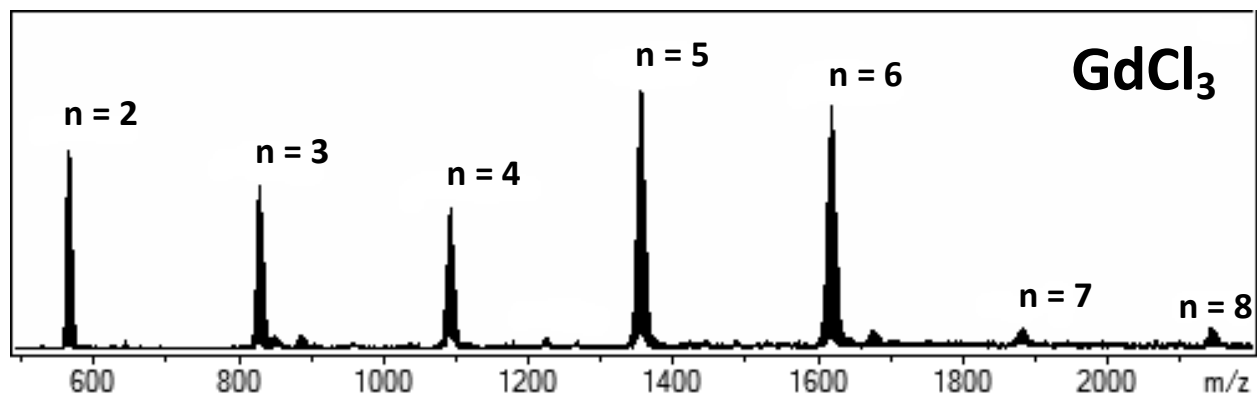


Figure S1g. ESI mass spectra of 350 μM GdCl_3 in isopropanol. $\text{Gd}_n\text{Cl}_{3n+1}^-$ clusters are labeled.

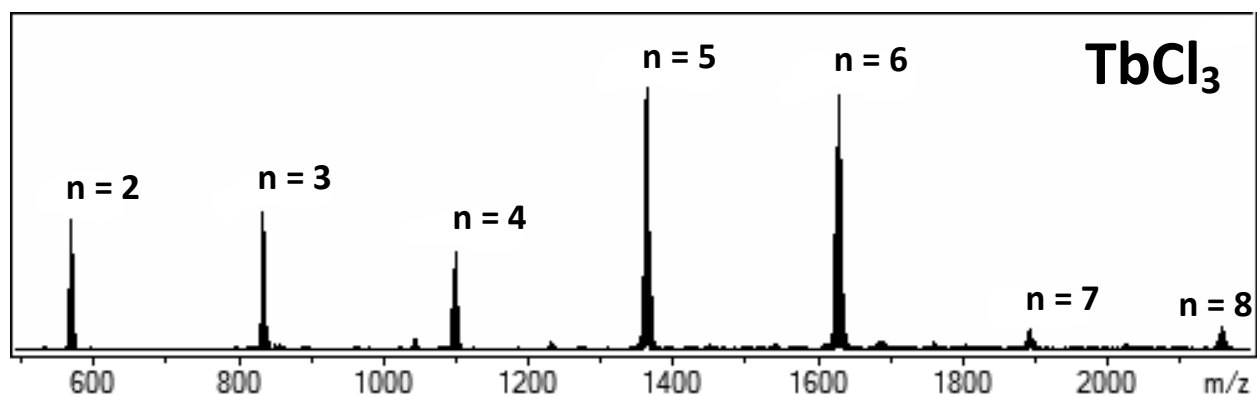


Figure S1h. ESI mass spectra of 350 μM TbCl_3 in isopropanol. $\text{Tb}_n\text{Cl}_{3n+1}^-$ clusters are labeled.

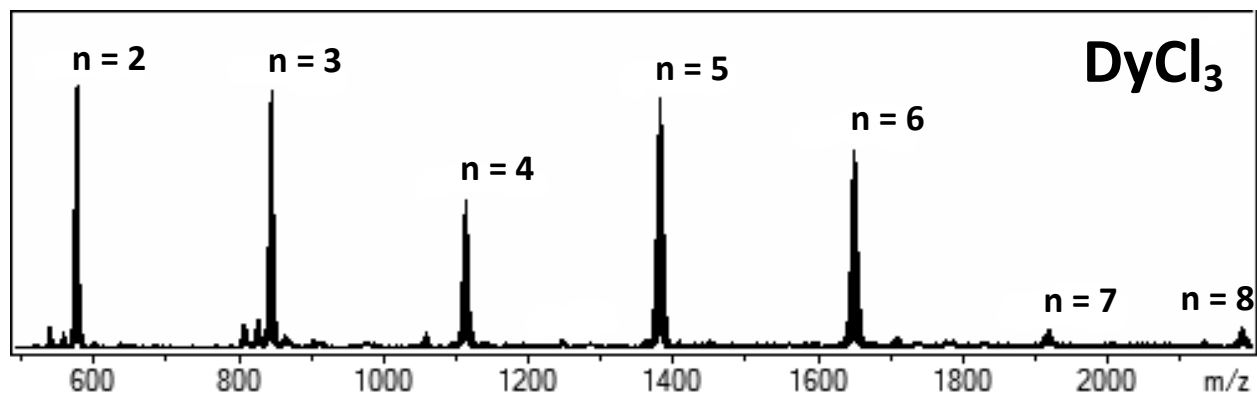


Figure S1i. ESI mass spectra of 350 μM DyCl_3 in isopropanol. $\text{Dy}_n\text{Cl}_{3n+1}^-$ clusters are labeled.

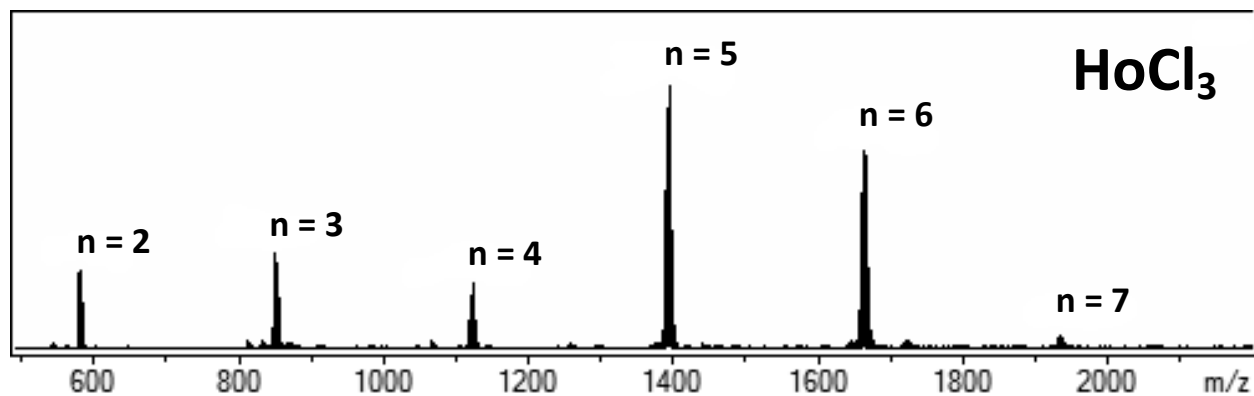


Figure S1j. ESI mass spectra of 350 μM HoCl_3 in isopropanol. $\text{Ho}_n\text{Cl}_{3n+1}^-$ clusters are labeled.

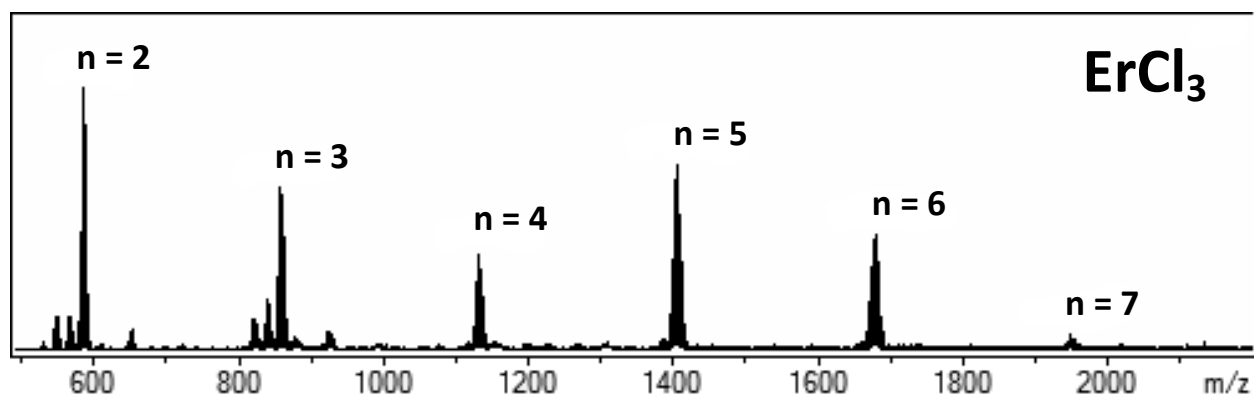


Figure S1k. ESI mass spectra of 350 μM ErCl_3 in isopropanol. $\text{Er}_n\text{Cl}_{3n+1}^-$ clusters are labeled.

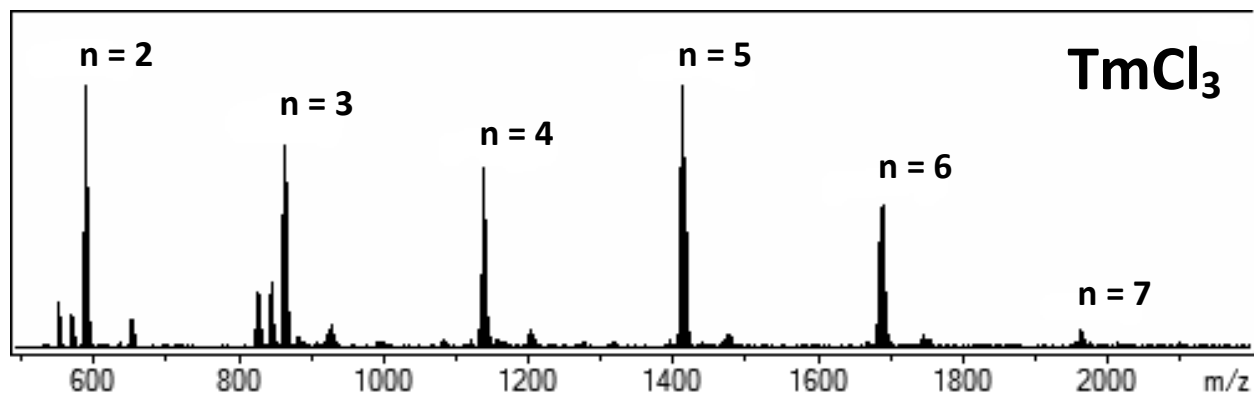


Figure S1l. ESI mass spectra of 350 μM TmCl_3 in isopropanol. $\text{Tm}_n\text{Cl}_{3n+1}^-$ clusters are labeled.

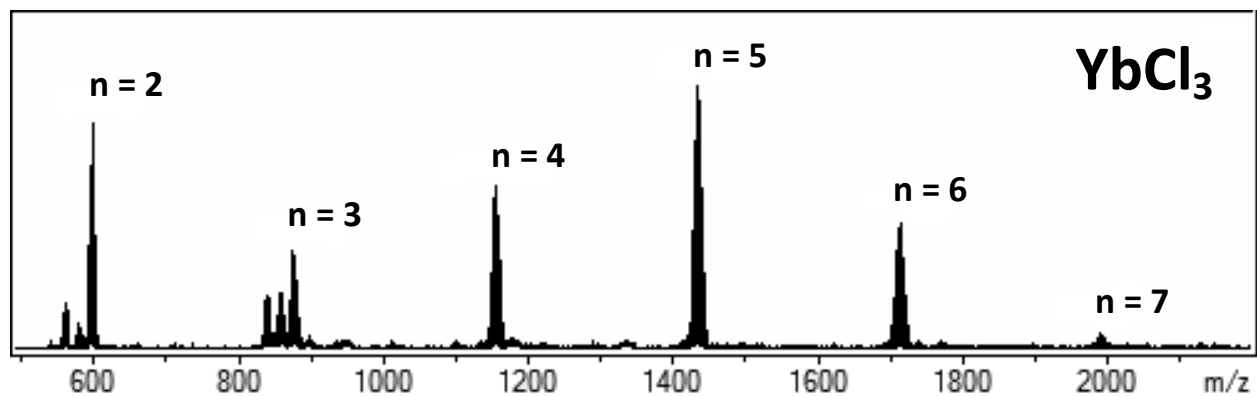


Figure S1m. ESI mass spectra of 350 μM YbCl_3 in isopropanol. $\text{Yb}_n\text{Cl}_{3n+1}^-$ clusters are labeled.

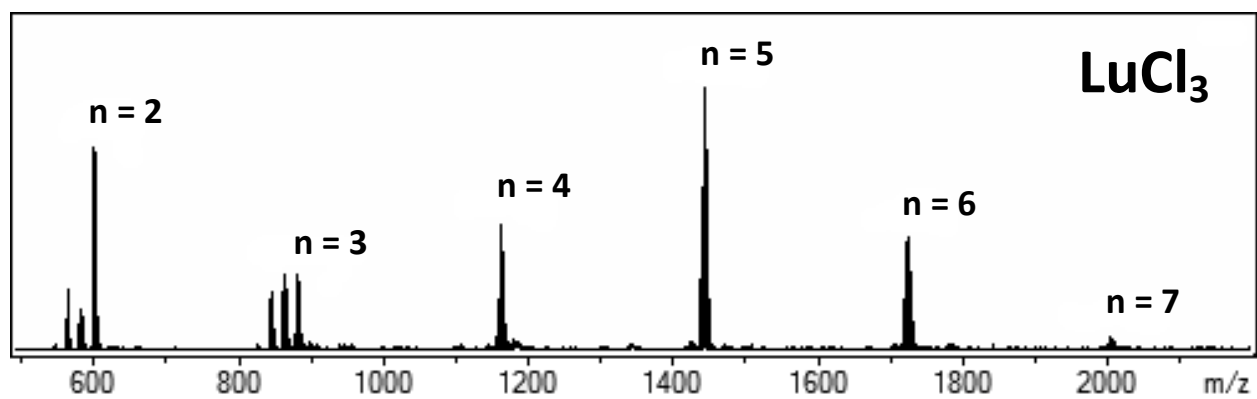


Figure S1n. ESI mass spectra of 350 μM LuCl_3 in isopropanol. $\text{Lu}_n\text{Cl}_{3n+1}^-$ clusters are labeled.

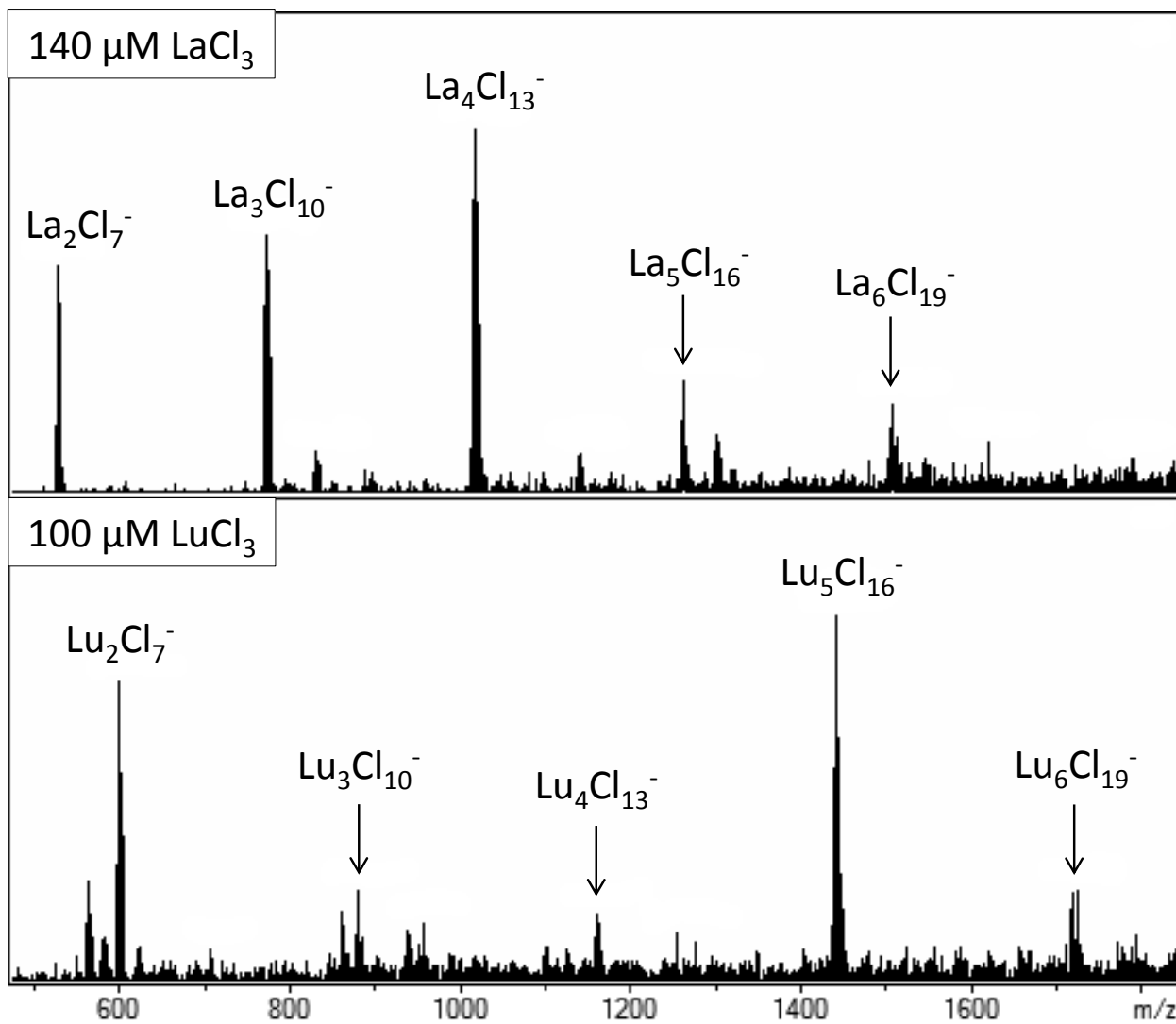


Figure S2. ESI mass spectra of 140 μM LaCl₃ (top) and 100 μM LuCl₃ (bottom) in isopropanol. The signal-to-background ratio is inferior to that for the more concentrated 350 μM solutions, but the same “magic number” compositions, La₄Cl₁₃⁻ and Lu₅Cl₁₆⁻, are clearly apparent.

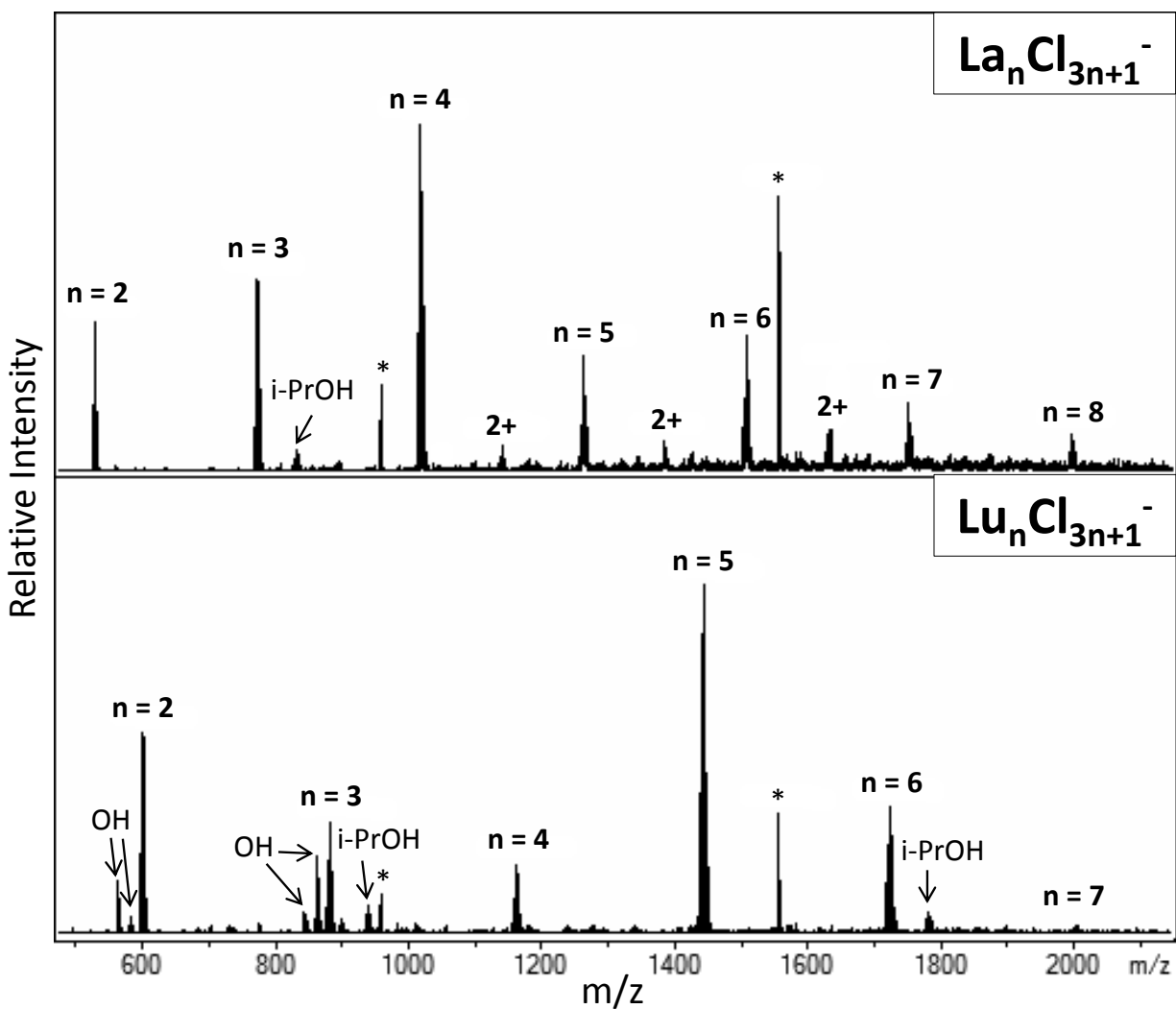
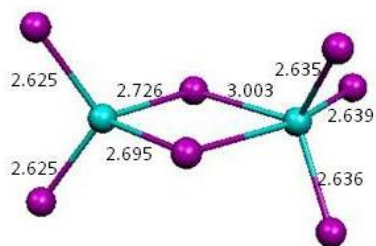
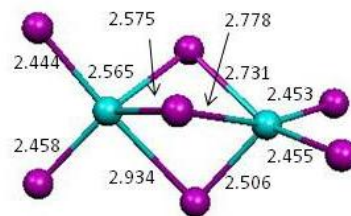


Figure S3. ESI mass spectra of 350 μM LaCl_3 (top) and LuCl_3 (bottom) in isopropanol, with the chloride concentration increased to 10.35 mM by addition of HCl, to a concentration of 10 mM. The “magic number” compositions, $\text{La}_4\text{Cl}_{13}^-$ and $\text{Lu}_5\text{Cl}_{16}^-$, remain clearly evident upon increasing the Cl^- concentration by $\sim 30\times$, from 0.35 mM in the other studied solutions to 10.35 mM in these solutions. The peaks identified by asterisks which appear in both mass spectra are unidentified impurities which do not exhibit isotopic patterns corresponding to incorporation of $^{35}\text{Cl}/^{37}\text{Cl}$. Peaks corresponding to addition of isopropanol, and to chloride substitution by hydroxide, are identified.



La_2Cl_7^-
RE = 11 kJmol^{-1}



Lu_2Cl_7^-
RE = 5 kJmol^{-1}

Figure S4. Geometric structures of higher-energy isomers of La_2Cl_7^- and Lu_2Cl_7^- . Relative energies (RE) are calculated with respect to the ground-state structures.

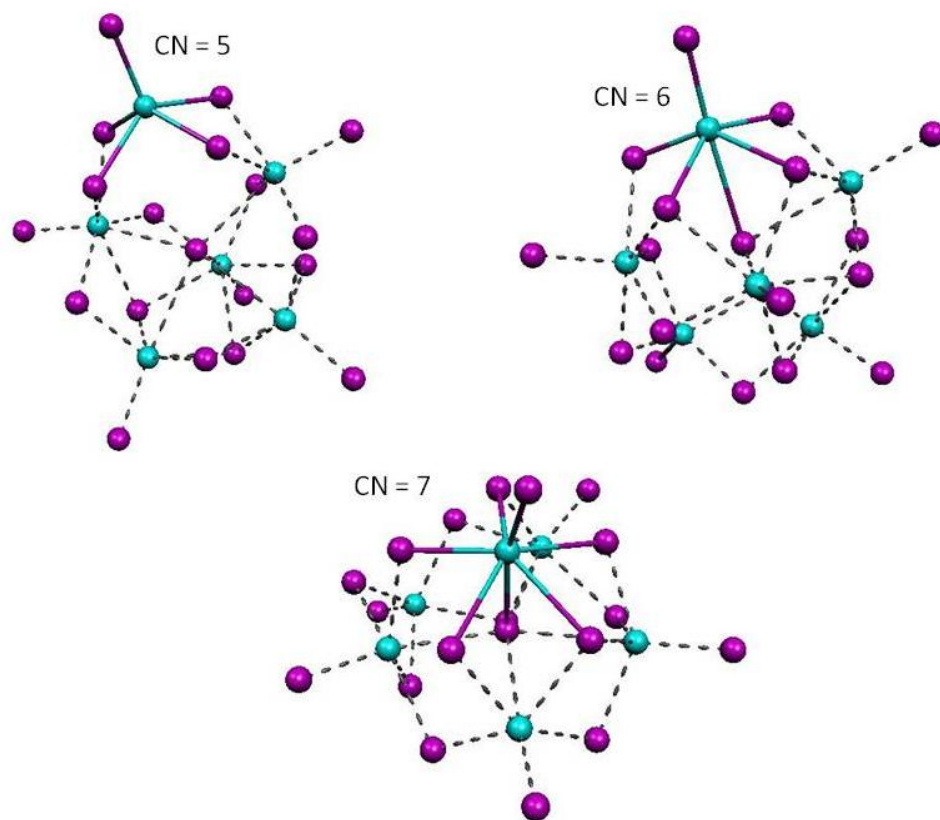


Figure S5. Different views of $\text{La}_6\text{Cl}_{19}^-$ showing different lanthanide coordination numbers.

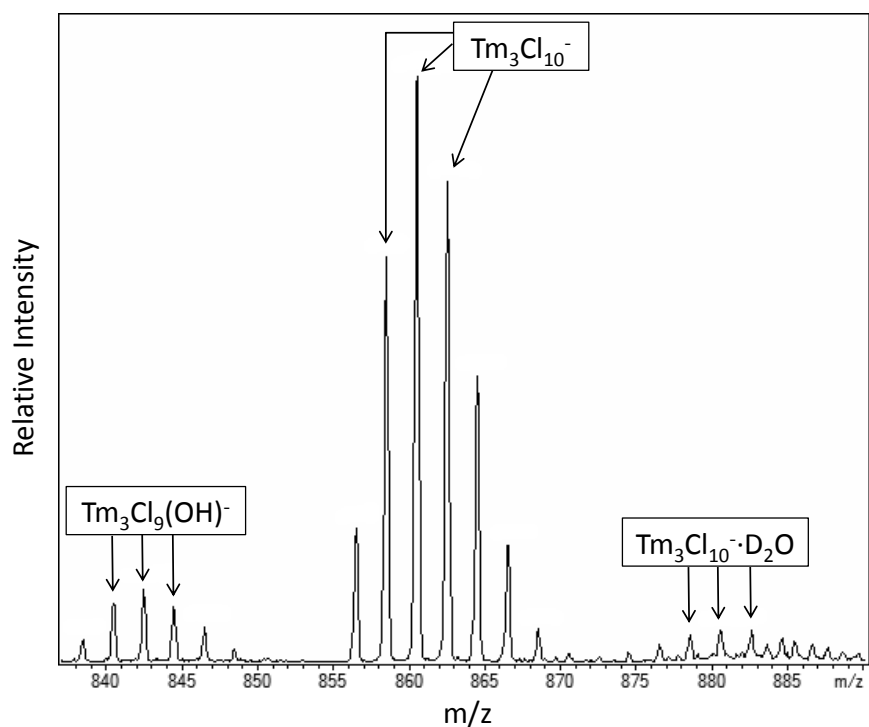
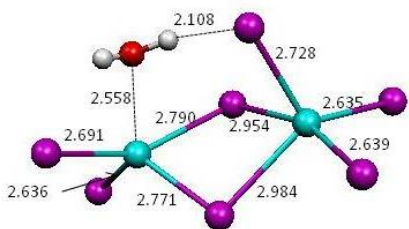
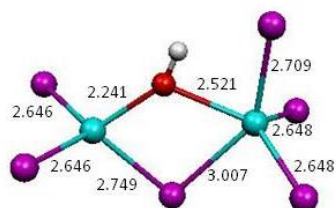


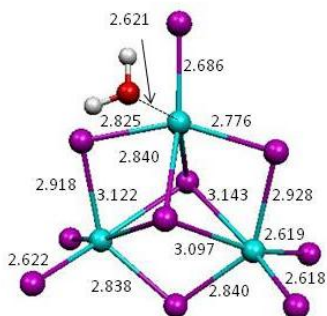
Figure S6. Portion of ESI mass spectrum of a solution of 350 μM TmCl_3 in 1% D_2O /99% $(\text{CH}_3)_2\text{CH}(\text{OD})$ showing $\text{Tm}_3\text{Cl}_{10}^-$ and its hydration and hydrolysis products. For each species the three m/z peaks calculated as most intense are indicated by arrows.



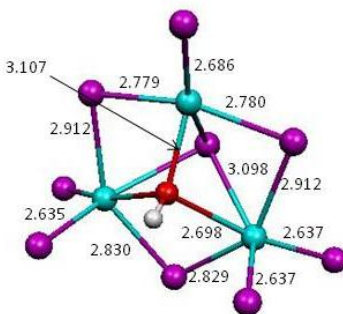
$\text{La}_2\text{Cl}_7(\text{H}_2\text{O})^-$



$\text{La}_2\text{Cl}_6\text{OH}^-$



$\text{La}_3\text{Cl}_{10}(\text{H}_2\text{O})^-$



$\text{La}_3\text{Cl}_9\text{OH}^-$

Figure S7. Hydration and hydrolysis products of La_2Cl_7^- and $\text{La}_3\text{Cl}_{10}^-$.

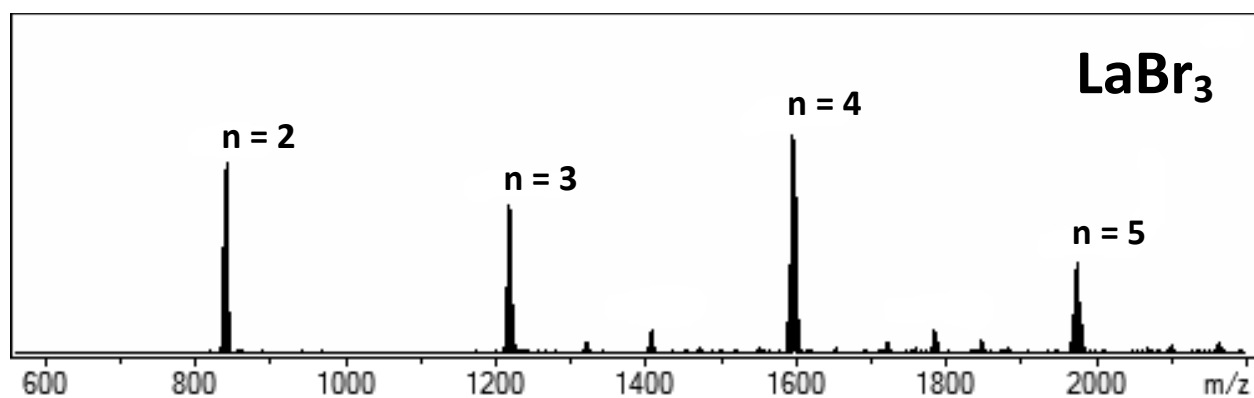


Figure S8a. ESI mass spectra of LaBr_3 in isopropanol. $\text{La}_n\text{Br}_{3n+1}^-$ clusters are labeled.

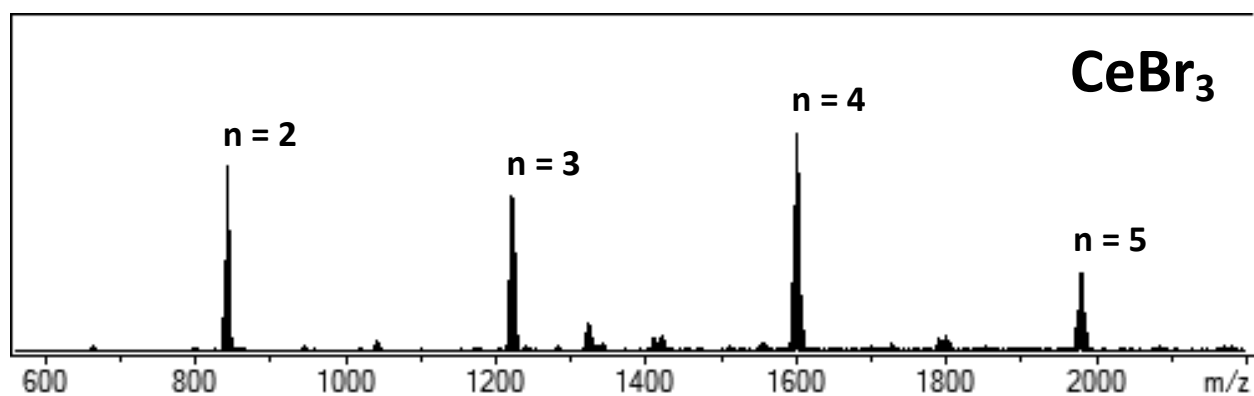


Figure S8b. ESI mass spectra of CeBr_3 in isopropanol. $\text{Ce}_n\text{Br}_{3n+1}^-$ clusters are labeled.

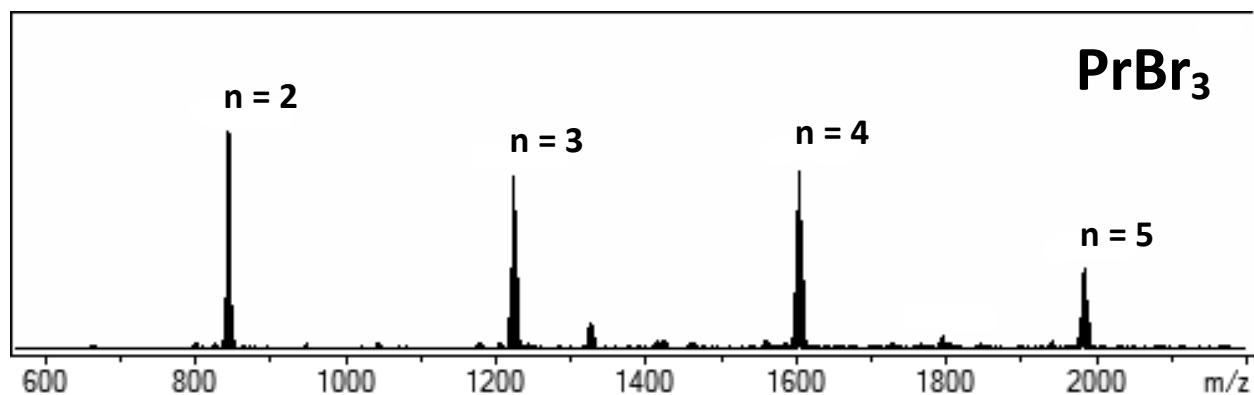


Figure S8c. ESI mass spectra of PrBr_3 in isopropanol. $\text{Pr}_n\text{Br}_{3n+1}^-$ clusters are labeled.

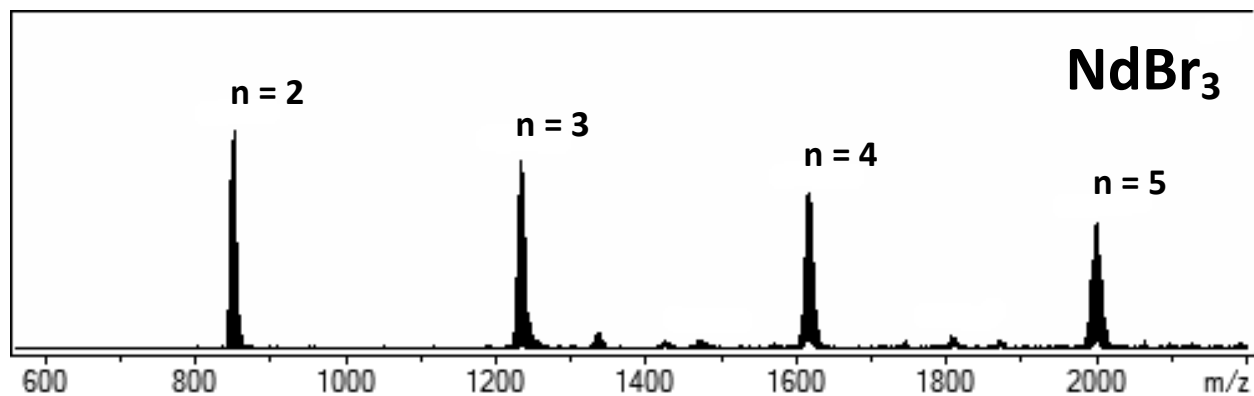


Figure S8d. ESI mass spectra of NdBr_3 in isopropanol. $\text{Nd}_n\text{Br}_{3n+1}^-$ clusters are labeled.

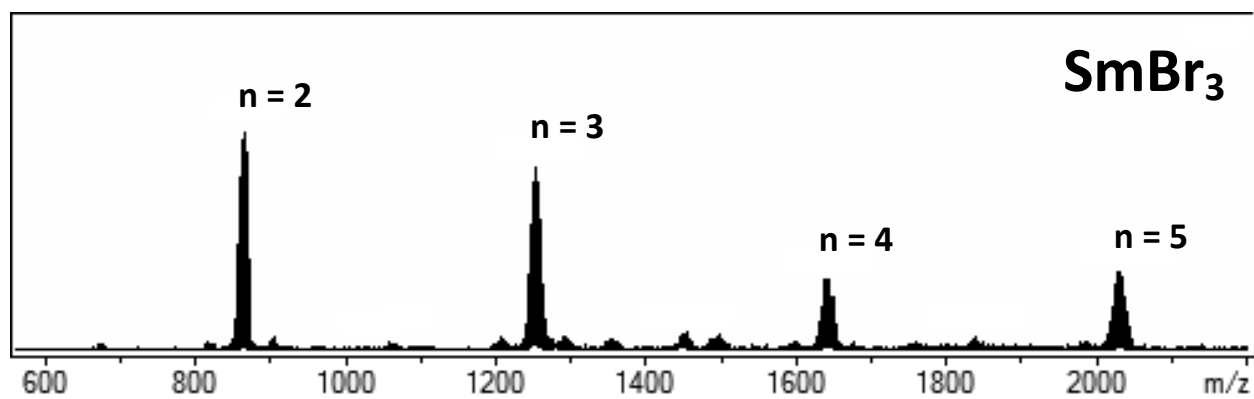


Figure S8e. ESI mass spectra of SmBr_3 in isopropanol. $\text{Sm}_n\text{Br}_{3n+1}^-$ clusters are labeled.

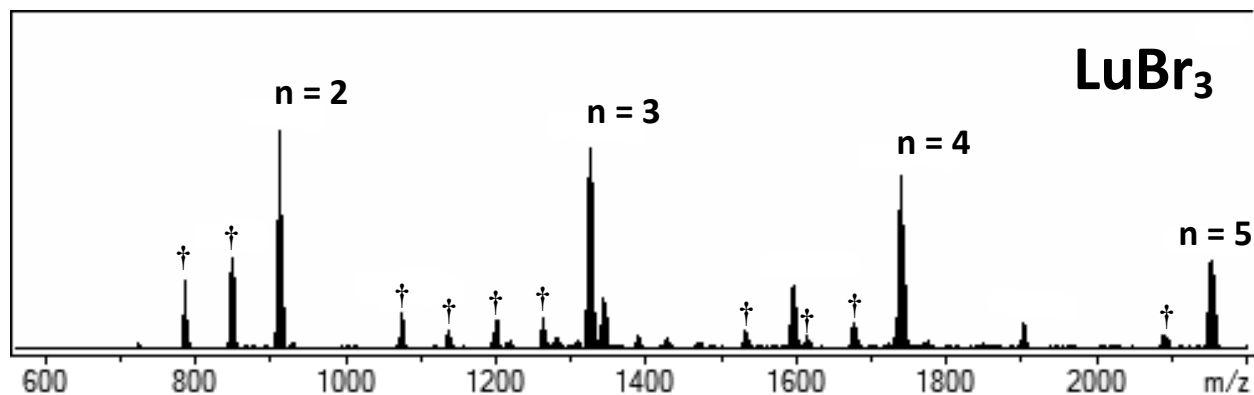


Figure S8f. ESI mass spectra of LuBr_3 in isopropanol. $\text{Lu}_n\text{Br}_{3n+1}^-$ clusters are labeled. Hydroxide-substituted clusters are indicated by daggers.

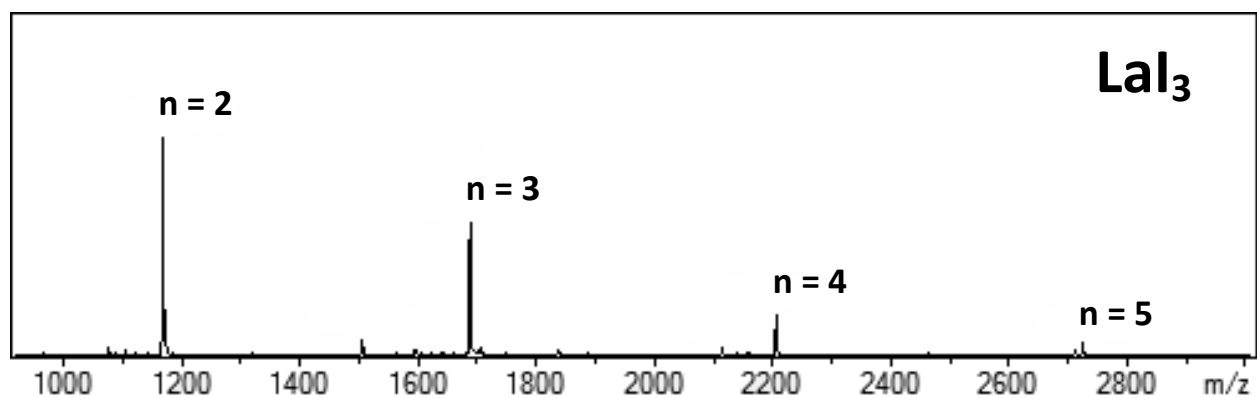


Figure S9a. ESI mass spectra of LaI_3 in isopropanol. $\text{La}_n\text{I}_{3n+1}^-$ clusters are labeled.

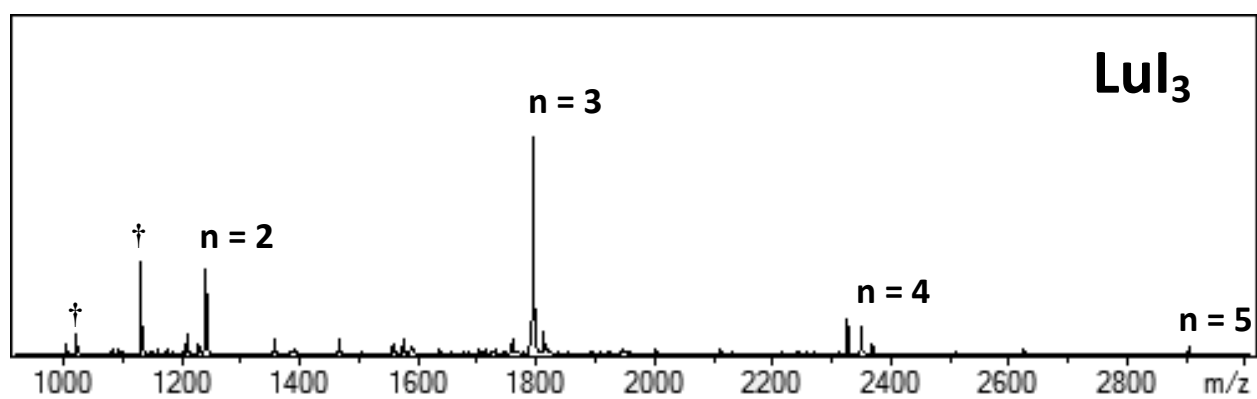


Figure S9b. ESI mass spectra of LuI_3 in isopropanol. $\text{Lu}_n\text{I}_{3n+1}^-$ clusters are labeled. Hydroxide-substituted clusters are indicated with daggers.

Table S1. AIM Charges for LaCl_3 and $\text{La}_n\text{Cl}_{3n+1}^-$ ($n=1-6$) clusters

	La	Cl (terminal) ^a	Cl (bridge) ^a	Cl (center) ^a
LaCl_3	1.963	-0.654	-	-
LaCl_4^-	1.975	-0.744	-	-
La_2Cl_7^-	1.998	-0.716	-0.711	-
$\text{La}_3\text{Cl}_{10}^-$	1.994	-0.695	-0.700	-
$\text{La}_4\text{Cl}_{13}^-$	2.011	-0.688	-0.695	-0.730
$\text{La}_5\text{Cl}_{16}^-$	2.019	-0.672	-0.689	-0.759
$\text{La}_6\text{Cl}_{19}^-$	1.993	-0.664	-0.689	-0.761

^a Averaged values over all the corresponding Cl atoms.

Table S2. AIM Charges for LuCl_3 and $\text{Lu}_n\text{Cl}_{3n+1}^-$ ($n=1-6$) clusters

	Lu	Cl (terminal) ^a	Cl (bridge) ^a	Cl (center) ^a
LuCl_3	2.009	-0.670	-	-
LuCl_4^-	1.979	-0.745	-	-
Lu_2Cl_7^-	2.013	-0.703	-0.754	-
$\text{Lu}_3\text{Cl}_{10}^-$	2.007	-0.697	-0.707	-
$\text{Lu}_4\text{Cl}_{13}^-$	2.042	-0.694	-0.707	-0.738
$\text{Lu}_5\text{Cl}_{16}^-$	2.012	-0.679	-0.689	-0.764
$\text{Lu}_6\text{Cl}_{19}^-$	2.010	-0.676	-0.686	-0.777

^a Averaged values over all the corresponding Cl atoms.

Table S3. Lanthanide bromide cluster abundances normalized to the most abundant cluster for each lanthanide.^a

	2	3	4	5
La_nBr_{3n+1}⁻	65%	59%	100%	45%
Ce_nBr_{3n+1}⁻	65%	63%	100%	40%
Pr_nBr_{3n+1}⁻	95%	85%	100%	50%
Nd_nBr_{3n+1}⁻	87%	100%	98%	91%
Sm_nBr_{3n+1}⁻	95%	100%	45%	53%
Lu_nBr_{3n+1}⁻	100%	95%	80%	42%

^a Cluster abundances correspond to the sum of peak intensities for all isotopomers which contribute to the isotopic distribution for a given cluster composition. Only Lu₂Br₇⁻ and Lu₃Br₁₀⁻ hydrolyzed; the contributions from the OH-substituted clusters are included.